Disruption of zinc (II) binding and dimeric protein structure of the XIAP-RING domain by copper (I) Ions

Kathryn E. Splan,✉ Sylvia R. Choi, Ruth E. Claycomb, Isaiah K. Eckart-Frank, Shreya Nagdev, and Madeline E. Rodemeier

Department of Chemistry, Macalester College, 1600 Grand Avenue, Saint Paul, MN 55105
✉ Corresponding author: Tel; 651-696-6109. Fax: 651-696-6432. Email: splank@macalester.edu

Submitted to *Journal of Biological Inorganic Chemistry*, November 16, 2022
Revised February 9, 2023

Abstract

Modulation of metalloprotein structure and function via metal ion substitution may constitute a molecular basis for metal ion toxicity and/or metal-mediated functional control. The X-linked Inhibitor of Apoptosis Protein (XIAP) is a metalloprotein that requires zinc for proper structure and function. In addition to its role as a modulator of apoptosis, XIAP has been implicated in copper homeostasis. Given the similar coordination preferences of copper and zinc, investigation of XIAP structure and function upon interaction with copper is relevant. The Really Interesting New Gene (RING) domain of XIAP is representative of a class of zinc finger proteins that utilize a bi-nuclear zinc binding motif to maintain proper structure and ubiquitin ligase function. Herein, we report the characterization of copper (I) binding to the Zn_2-RING domain of XIAP. Electronic absorption studies that monitor copper-thiolate interactions demonstrate that the RING domain of XIAP binds 5-6 Cu(I) ions and that copper is thermodynamically preferred relative to zinc. Repetition of the experiments in the presence of the Zn(II)-specific dye Mag-Fura2 shows that Cu(I) addition results in Zn(II) ejection from the protein, even in the presence of glutathione. Loss of dimeric structure of the RING domain, which is a requirement for its ubiquitin ligase activity, upon copper substitution at the zinc binding sites, was readily observed via size exclusion chromatography. These results provide a molecular basis for the modulation of RING function by copper and add to the growing body of literature that describe the impact of Cu(I) on zinc metalloprotein structure and function.

Keywords: copper, zinc finger, metalloprotein, X-linked inhibitor of Apoptosis, RING

Graphical Abstract

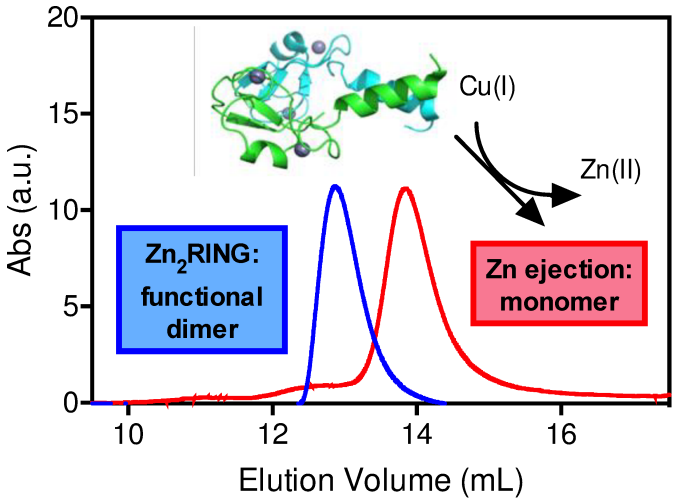

Introduction

Numerous biological processes require copper ions, but at elevated levels copper exhibits toxicity to all cells. Therefore, nature has optimized copper homeostasis pathways to ensure that cellular copper concentrations are appropriately maintained and that the ion binds to its intended target [1-3]. However, subtle differences in coordination preferences that dictate metal ion specificity may allow different metal ions to interact with binding sites, thereby modulating protein function. For example, elevated metal ion levels and/or dysfunction in copper ion homeostasis mechanisms can lead to mis-metalation of proteins and result in cellular toxicity [4, 5]. From a functional perspective, a role for transition-metal ions in signaling has emerged, in which copper and other metal ion fluxes promote signaling pathways, often by binding to other biomolecules [6-8]. Given the possibilities associated with metal-ion binding, it is therefore important to have a broad understanding of the interaction of copper and other metals with their functional targets as well as others proteins and biomolecules that exhibit similar coordination preferences.

Zinc finger (ZF) proteins constitute an important class of metalloproteins that employ a combination of cysteine (C) and histidine (H) residues to bind Zn(II) as a structural element [9-11]. While ZFs were initially characterized as DNA-binding transcription factors, the term “zinc finger” is more commonly used to describe any small, independently folded domain that requires one or more zinc ions to assume proper structure [12]. As defined, ZFs exhibit many functions including DNA and RNA recognition, apoptosis regulation, and protein ubiquitination, and it is estimated that over 3% of the proteins in the human genome can be characterized as ZFs [13], highlighting the importance of this class of proteins. While all ZFs exhibit a Zn(II) tetrahedral coordination geometry, the overall protein fold stabilized upon zinc coordination is diverse, with the resulting domain folds currently classified into over 14 groups [14]. Despite the preferred coordination for Zn(II), other metals with moderate to high affinity for thiolate and nitrogen ligands also bind to zinc finger domains, including Pb (II) [15], Fe(II) [16, 17], Cd(II) [18, 19] [20], Ni(II) [17, 21], Co(II) [22-24], Cu(II) [25-28], Au(I) [29-31], and Ag [32-34]. The ability of multiple metal ions to interact with ZF domains provides a putative molecular basis for metal ion toxicity of environmentally hazardous metals and metal-based nanoparticles. Similarly, ZF domains have received considerable attention as targets for metal-based drugs [35, 36].

Both Cu(I) and Zn(II) are thiophilic ions with a d^{10} electron configuration, and given the predominance of reduced copper under biological conditions, the interaction of Cu(I) with thiol-rich metal binding sites such as those found in ZF proteins is of fundamental interest. In this context, we and others have studied the impact of Cu(I) on ZF structure and function. Cu(I) can readily bind to apo-ZF peptides that adopt the classical $\beta\beta\alpha$ secondary structural motif, the NCp7 peptide that constitutes the C-terminal "zinc knuckle" domain of the HIV nucleocapsid protein, and one and two domain constructs of the non-classical ZF protein tristetraprolin (TTP). Moreover, addition of Cu(I) to Co(II)- and/or Zn(II)-reconstituted peptides results in metal ion displacement by copper, demonstrating that Cu(I) has a high affinity for ZF binding sites with diverse coordination motifs [37-39]. However, the relative susceptibility of ZF domains toward Cu(I) substitution and resulting metal-bound species are likely variable. For example, Cu(I) substitution significantly alters the structure of the consensus peptide CP-CCHC but not the second ZF domain of Sp1, both of which display the classical ZF structure when bound to Zn(II) [37, 39]. Similarly, Sommer et al. showed that Cu(I) can replace Zn(II) from the non-classical ZF domains of *Chlamydomonas reinhardtii* copper response regulator 1 (CCR1) with little impact on structure, as gauged by circular dichroism measurements, while Cu(I) impacts both the structure and function of the ZF domains in tristetraprolin (TTP) [38, 40]. These results demonstrate that the impact of Cu(I) substitution on the structure and function of ZF domains is not well understood.

To further our understanding of the impact of Cu(I) on ZF structure and function, our work herein focuses on copper interactions with the Really Interesting New Gene (RING) finger domain of the anti-apoptotic protein X-linked Inhibitor of Apoptosis Protein (XIAP). In addition to its role in apoptosis, XIAP has been implicated to play a role in copper homeostasis. Specifically, the ubiquitination activity of the RING domain of XIAP results in degradation of COMMD1, a copper-binding protein associated with copper export [41, 42]. Cellular levels of XIAP expression decrease under elevated copper levels, resulting in a putative feedback loop wherein increasing copper levels correlate with higher COMMD1 expression and hence, copper export. XIAP features four zinc-binding domains: three baculovirus repeat (BIR) domains and a C-terminal RING domain. Each BIR domain binds one Zn(II) ion via a three Cys one His motif while the RING domain constitutes a bi-nuclear Zn(II) motif (Figure 1), and the displacement of Zn(II) by Cu(I) is one possible mechanism by which copper could modulate XIAP function. We and others have shown that

copper interacts at surface accessible binding sites on the BIR domains in XIAP constructs lacking the RING domain, and that the zinc structural sites of the BIR domains are not the primary copper-binding sites [43, 44].

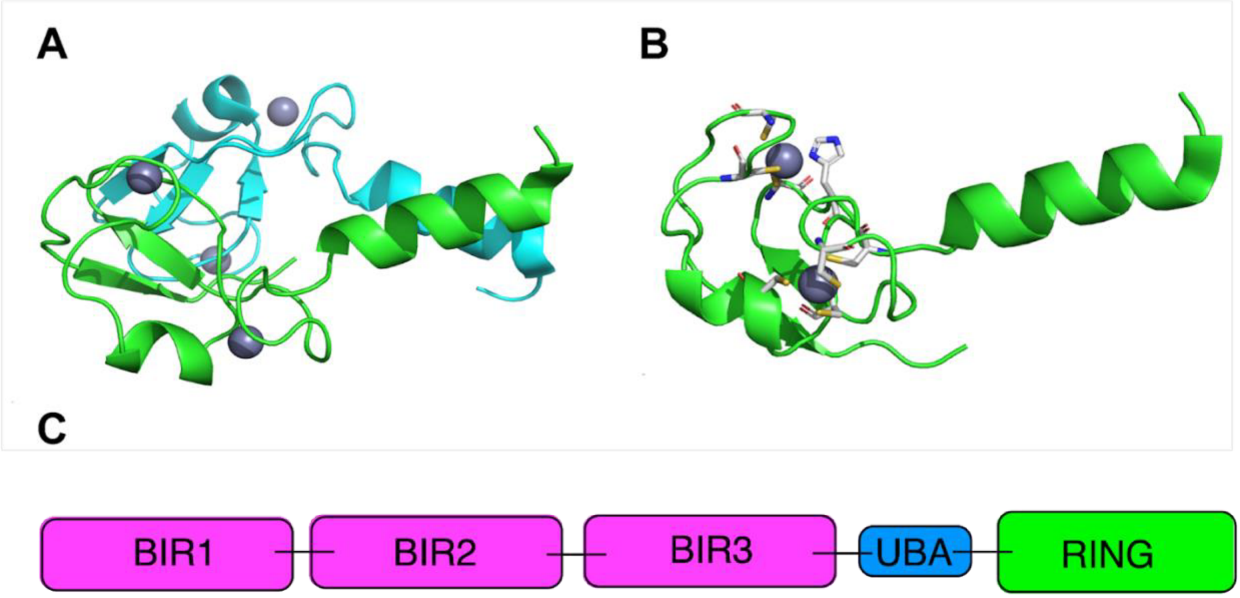

Figure 1. Crystal structure of the dimeric RING domain of E3 ubiquitin-protein ligase XIAP generated via PyMOL (PDB: 4IC2). The Zn(II) ions are shown in gray. The two monomers are differentiated by color. **B.** ZFs site of the monomeric RING protein. One zinc ion is coordinated to a CCHC ligand set (top) and the other is coordinated to CCCC (bottom). **C.** Protein domain map of the full-length XIAP protein.

Herein we extend our investigation of XIAP-copper interactions to the RING domain. RING domains constitute a class of ZF proteins that contain a bi-nuclear Zn(II) motif with a characteristic linear sequence of Cys-X_2-Cys-X_{9-39}-Cys-X_{1-3}-His-X_{2-3}-Cys(His)-X_2-Cys-X_{4-48}-Cys-X_2-Cys [45-47]. The domain binds two zinc ions wherein the two tetrahedral binding sites are made up of the first and third and second and fourth ligand pairs. Mutation of His467 to alanine within the XIAP RING domain results in loss of ubiquitination activity, demonstrating that proper metal binding is required for activity [48]. By extension, Cu(I) binding within the zinc sites may alter domain structure and impact RING domain function. Therefore, a thorough understanding of Cu(I) interactions with this domain is critical for the elucidation of plausible mechanisms by which copper may modulate the ubiquitination function of XIAP and by extension, other RING-containing proteins in this family. While this work was in progress, Wang et al. reported on the interaction of Cu(I) with the RING finger domain of RNF11, which also functions as an E3 ligase within numerous signaling pathways but maintains a different ligand set and overall tertiary structure when compared to the XIAP

RING domain [49]. Taken together, these studies provide insight into multiple RING domains' susceptibility to modulation by copper (I) ions.

Material and Methods

Materials.

All reagents were from Sigma-Aldrich unless otherwise noted. *E. coli* cloning and expressions strains, Phusion polymerase, DpnI, and deoxynucleotides were from New England Biolabs.

Expression, purification, and characterization of XIAP-RING_F495W proteins.

A pGEX-4T-1 plasmid containing the gene for XIAP-RING residues 429-497 was purchased from Genscript. In the purchased construct, a tryptophan residue was introduced at position F495 to aid in concentration measurement, as it has previously been shown that the F495W variant maintains the structure and function of XIAP-RING [50]. The V461E mutation was introduced via PCR-based site-directed mutagenesis using Phusion polymerase followed by DpnI digestion of the template plasmid. The mutation was confirmed via DNA sequencing (University of Minnesota Genomics Center).

The resulting plasmids encoding for glutathione *S*-transferase (GST)-fusions RING variants were transformed into *E. coli* BL21(DE3), grown to mid-log phase at 37°C, induced with 0.1 mM isopropyl β-D-1-thiogalactopyranoside (IPTG) and 0.1 mM $ZnSO_4$ as a supplement, and then grown overnight at room temperature. For a 1 L culture, harvested cells were resuspended in sonication buffer (50 mM Tris pH 7.5, 100 mM NaCl) supplemented with PMSF and protease inhibitor tablets and lysed via sonication. The lysate was passed over glutathione sepharose 4B resin (2 mL; GE Healthcare Life Sciences/Cytiva) and washed with phosphate-buffered saline. The proteins were cleaved from the resin via treatment with thrombin (GE Healthcare Life Sciences/Cytiva) per manufacturer's protocol to yield the desired proteins with the GST tag removed. The mass of each protein was confirmed via mass spectrometry using a Waters Aquity Arc UHPLC with UV/Vis and QDa detector Liquid Chromatography Mass Spectrometer (LCMS) (Figure S2).

The extinction coefficient for the XIAP-RING_F495W construct used herein was determined via amino acid analysis on three independently purified protein samples (Molecular Structure Facility at University of California-Davis) to be 8,970 $M^{-1}cm^{-1}$ at 280 nm. Protein concentrations for all constructs were determined via absorbance measurements at 280 nm based upon this value. The number of Zn(II) ions

per protein upon purification was determined spectroscopically with the reagent 4-(2-pyridylazo)resorcinol (PAR). Protein samples (5-15 μM) were incubated for 18 hours in the presence of PAR (0.5 mM), iodoacetamide (0.9 mM) and guanidine-HCl (4 M) in 100 mM Hepes pH 7.5. [Zn(II)] was determined via absorption at 500 nm (Varian Cary 50 spectrophotometer) utilizing a calibration curve constructed from a 1 mM Zn(II) solution under the same conditions.

Spectroscopic measurements.

All buffers used for spectroscopic measurements were prepared from chelex-treated water. Measurements involving Cu(I) were conducted in an anaerobic chamber (Coy Laboratory Products) maintained with 95 % N_2/5 % H_2, unless otherwise noted. Cu(I) stock solutions were prepared in the anaerobic chamber by dissolving tetrakis(acetonitrile)copper(I) hexafluorophosphate in acetonitrile. The Cu(I) concentration was determined spectroscopically by addition of known amounts of the stock to 1mM bathocuproinedisulfonic acid (BCS) to form $Cu(BCS)_2$ ($\varepsilon_{483\ nm}$ = 12,500 $M^{-1}cm^{-1}$) [51]. All experiments, including measurement of Cu(I) stock solutions, were performed in 50 mM Hepes pH 7.5, 150 mM NaCl unless otherwise stated.

Absorption spectra were recorded with an Agilent 8453 spectrophotometer in either small volume quartz cuvettes (Starna, Inc.) or 1.0 mL disposable cuvettes (BrandTech Scientific, Inc). To measure Cu(I) binding to XIAP-RING-W, ~ 10 μM of protein in 1.0 mL buffer was titrated with increasing equivalents of Cu(I). added from a freshly prepared Cu(I) solution in 5% acetonitrile diluted from the stock solution described above. Care was taken to ensure that the total volume of added copper solution did not exceed 10 % of the initial volume, and when absorbance changes were plotted as a function of copper concentration, the concentration of the copper was corrected for dilution. Experiments were performed both in the absence and presence of the zinc specific indicator Mag-Fura-2 (50 μM) (ThermoFischer). Care was taken to ensure that spectral changes were complete before recording the final spectra data, which in all cases, were within 1-2 minutes of addition of the aliquot. To obtain the relative affinity of copper and zinc for the protein, titration data were fit to the following binding isotherm [52]:

$$f = \frac{A - A_o}{A_{max} - A_o} = \frac{K_{obs} + P_T + M_T - \sqrt{(K_{obs} + P_T + M_T)^2 - 4P_T M_T}}{2P_T}$$

where the fractional binding (*f*) is calculated from absorbance data and M_T is the concentration of added copper, P_T is the total concentration of copper binding sites, and K_{obs} represents the equilibrium constant for the following metal exchange reaction:

$$2Zn(II) + Cu_nRING \rightarrow nCu(I) + Zn_2RING$$

wherein n = number of Cu(I) ions bound, rather than for the dissociation of copper from XIAP-RING-W.

Cu:XIAP-RING-W stoichiometry was estimated via a combined BCS/Bradford assay. 50 μM XIAP-RING-W was incubated in the presence of 10 equivalents of Cu(I) and 2 mM ascorbate under anaerobic conditions for 30 min. After incubation the sample was removed from the chamber and applied to a Micro-Biospin P6 column (BioRad) to separate un-bound and weakly bound Cu(I) per the manufacturer's instructions. Following centrifugation, the filtrate containing copper-bound protein was analyzed for protein and copper concentration. The protein concentration was determined via the Bradford assay using known concentrations of XIAP-RING-W as a standard. [Cu(I)] concentration was determined spectrophometrically using BCS in 50 mM Hepes buffer containing the 2.5 M guanidinium hydrochloride and 2 mM ascorbate to ensure unfolding of the protein and removal of Cu(I) by BCS.

Analytical Size Exclusion Chromatography.

Analytical size exclusion measurements were performed on a Superdex 75 10/300 GL column (GE Healthcare Life Sciences) attached to an UPC-900 AKTA FPLC system in 50 mM Hepes pH 7.5 and 150 mM NaCl. The column was calibrated with blue dextran (2000 kD), conalbumin (75 kD), ovalbumin (44 kD) carbonic anhydrase (29 kD), ribonuclease A (13.7 kD), and aprotinin (6.5 kD) all obtained from GE Healthcare Life Sciences. Protein concentration was 42 μM for all samples, and other components were added as indicated. Samples containing Cu(I) were prepared under anaerobic conditions in the glovebox, and 2 mM ascorbate was included to facilitate the presence of Cu(I) under ambient conditions during the course of the experiment.

To assess the stability of Cu(I) during the course of the SEC measurements, 300 μM samples of Cu(I) were prepared in degassed buffer in the absence and presence of 2 mM ascorbate. Each sample was then exposed to ambient conditions. At the time points indicated, the Cu(I) concentration was determined upon the addition of 100 μl of the solution to a cuvette containing 1mM bicinchoninic acid (BCA) to form $Cu(BCA)_2$ ($\varepsilon_{562\ nm}$ = 7,900 $M^{-1}cm^{-1}$) [53] in a final volume of 1.0 mL. To assess the stability of Cu(I)

bound to the RING protein under ambient conditions, 50 μM copper was added to 10 μM XIAP-RING in degassed buffer. The sample was exposed to ambient conditions and the electronic absorption spectrum was recorded as a function of time as indicated.

Results and Discussion

Preparation of Protein Variants

In order to characterize the metal-binding properties of XIAP-RING we utilized a construct containing residues 429-497 as well as the mutation F495W to aid in concentration determination, referred to XIAP-RING-W throughout. Replacement of Phe 495 with either Tyr or Trp retains both the dimeric structure of the RING domain and its Ub transfer activity, ensuring that this construct is suitable to gauge the impact of Cu(I) binding on structure [50]. For reference in our size exclusion studies (see below), we also prepared XIAP-RING-W_V461E that exists in a monomeric, rather than dimeric quaternary structure [50]. Both proteins were expressed as GST fusions and isolated upon proteolytic cleavage from the GST resin according to standard protocols, and their identity was confirmed via mass spectrometry (Figure S2). Spectroscopic quantification of bound zinc upon treatment of the protein samples with guanidine hydrochloride and iodoacetamide in the presence of 4-(2-pyridylazo)resorcinol (Par) indicate both proteins purify with ~ 2 ions per monomeric protein unit (2.3 ± 0.2 for XIAP_RING-W and 2.0 ± 0.2 for the V461E variant; Figure S3). Moreover, size exclusion measurements (Table 1) indicate that the XIAP-RING-W construct retains its homodimeric structure, which is a previously identified feature of the XIAP and some other RING domains [45].

Electronic absorption spectroscopy of Cu(I) addition to XIAP-RING

The impact of Cu(I) on the RING domain of XIAP was explored using various spectroscopic experiments that were carried out to determine if Cu(I) interacts with XIAP-RING, if Cu(I) interacts with the metal binding regions of XIAP-RING, and to explore Cu(I) displacement of Zn(II). Cu(I) binding to XIAP-RING-W under anaerobic conditions was first monitored by measuring changes in the ultraviolet absorption spectrum since Cu(I)-thiolate interactions are correlated with absorbance features at wavelengths above 250 nm [37, 54]. The metal binding regions of XIAP-RING-W consist of seven cysteines and one histidine, and the only cysteine residues present in this variant of the protein are located at the zinc binding sites.

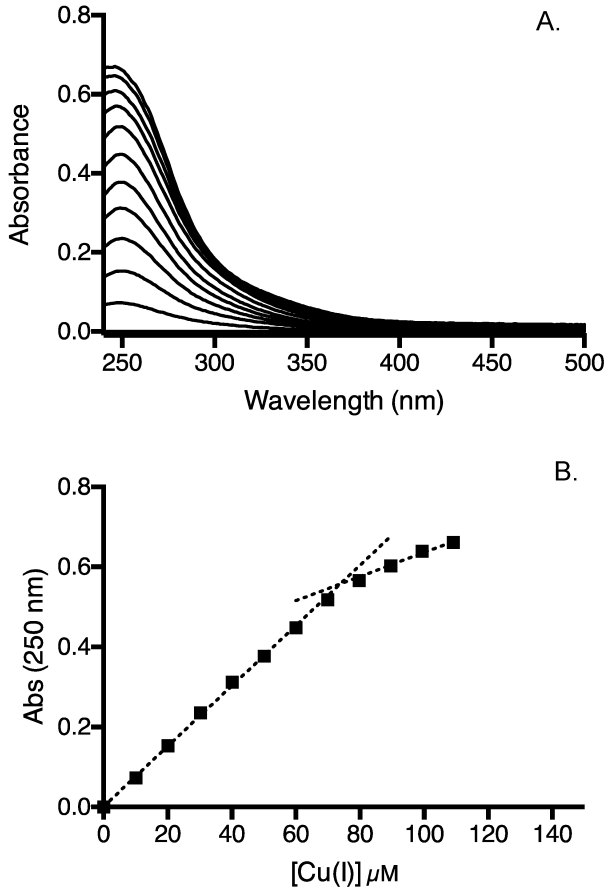

Figure 2. (A) Electronic absorption spectra upon addition of Cu(I) to 12.5 μM XIAP-RING-W measured in 50 mM HEPES, 150 mM NaCl, pH = 7.5. The spectrum of XIAP-RING-W prior to addition of copper has been subtracted. (B) Absorbance at 250 nm as a function of [Cu(I)].

Therefore, increases in absorbance in this region upon addition of Cu(I) is indicative of a metal binding interaction at the zinc-binding site. Addition of Cu(I) results in increased intensity in the ultraviolet region (Figure 2a), indicative of copper thiolate interactions (uncorrected spectra are shown in Figure S4). We note that the absorption changes observed closely resemble those seen when Cu(I) binds to other ZF holoproteins CCR1 [40] and RNF11 [49], which constitute other examples of Cu(I) binding to holo-ZF domains.

Monitoring the changes in absorption as a function of equivalents of copper over multiple trials and extrapolating the two linear regions reveals a distinct crossing point at 6.2 ± 0.4 equivalents of Cu(I) per RING domain. While the titration data are quite linear and indicate near-stoichometric binding, this does not necessarily indicate copper binding stoichiometry, given the need to compete with zinc. Moreover, it is possible that Cu(I) binds with significant affinity at other sites of the protein, further complicating elucidation of stoichiometry at the Zn(II) binding sites. To further probe the binding stoichiometry, 50 μM XIAP-RING-W was incubated in the presence of 10 equivalents of Cu(I) for 30 min. and the sample was purified with a spin column to remove weakly bound ions. Copper and protein concentrations were measured as described in the experimental sections to yield a Cu(I):RING ratio of (5.5 ± 0.5):1, further supporting the binding of multiple Cu(I) ions by XIAP-RING-W at the zinc binding sites and/or at other unspecified site(s) on the protein. Unfortunately, efforts to prepare apo-XIAP-RING-W by removal of bound zinc with EDTA under denaturing conditions and subsequent purification via reversed phase HPLC resulted in

insoluble peptide. Similarly, synthetic peptides that contain the zinc binding sites were difficult to obtain and upon purification resulted in low solubility that precluded quantitative binding studies with the apo-protein.

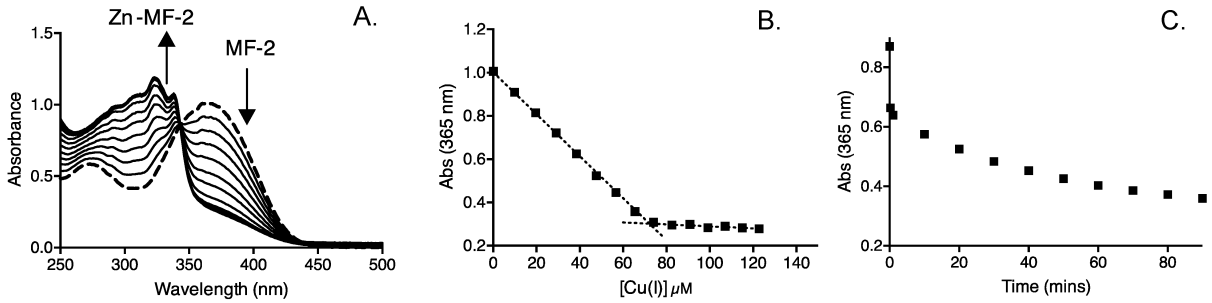

Figure 3. A: Electronic absorption spectra collected upon addition of Cu(I) to 15 μM XIAP-RING-W in the presence of 50 μM Mag-Fura-2. Spectra were measured in 50 mM HEPES, 150 mM NaCl, pH = 7.5. B: Absorbance at 365 nm as a function of added [Cu(I)]. C: Decrease in absorbance at 365nm as a function of time upon addition of addition of 70 μM Cu(I) to 15 μM XIAP-RING-W in the presence of 50 μM Mag-Fura-2 and 0.2 mM GSH.

The results presented above provide strong evidence for Cu(I) binding at the Zn(II) binding sites, but they do not demonstrate that Zn(II) is ejected from the protein nor do they rule out the possibility of mixed-metal species. Therefore, the above titration was repeated in the presence of Mag-Fura-2, which is a common spectroscopic probe for Zn(II). Specifically, when Zn(II) is added to Mag-Fura-2, the spectrum of the dye shifts substantially (Figure S5). Importantly, addition of Cu(I) results in far less spectral response, allowing for spectral changes to be correlated to released Zn(II). Titration of XIAP-RING-W with Cu(I) in the presence of Mag-Fura-2 results in a shift in the spectrum toward the Zn(II) complex in a concentration dependent manner (Figure 3a), suggesting that Cu(I) induces the release of Zn(II) from XIAP-RING-W. Monitoring the absorbance change that correlates to Zn(II) release as a function of Cu(I) equivalents indicates that zinc displacement is complete upon addition of 4.9 ± 0.3 Cu(I) equivalents. Again, the linearity of the absorbance changes as a function of added metal equivalents indicates the binding of multiple metal ions at the zinc-binding domain. Using the linear best fit line of absorbance versus [Zn(II)] (Figure S5) along with the initial absorbance of Mag-Fura-2 shows that 1.84 ± 0.04 equivalents of Zn(II) are displaced per RING protein throughout the course of the titration, consistent with the bi-nuclear zinc structure of the RING protein.

Further examination of the titration data suggests that copper binding is cooperative and likely does not progress through multiple, distinct copper complexes. For example, assuming that 2-3 Cu(I) ions

bind per metal binding site per the stoichiometries observed above, the linear increase in spectral response (Figure 2B) suggests that only one copper species is formed per metal binding site during the course of the titration. If multiple species were formed sequentially, increases in absorbance would likely be bi-phasic assuming each species has different spectral features. Cooperative binding by XIAP-RING-W is further supported by the observed linear Zn(II) release (Figure 3B) that requires 5 copper ions for completion. Sequential binding of copper at each zinc binding site would be likely result in complete Zn(II) release prior to saturation binding of copper. That 5 Cu(I) ions are required to fully release two bound Zn(II) ions argues against this scenario and further supports the cooperative nature of copper binding observed here. Finally, the linear increase in absorbance suggests that both metal binding sites within the RING exhibit similar spectral intensity owing to Cu(I)-thiolate coordination and/or they have highly similar affinity for copper, both of which are reasonable possibilities. This cooperative, rather than sequential, nature of copper binding could be further supported by titration studies followed by X-ray absorption spectroscopy that can directly report on the coordination properties of the resulting species, similar to those recently done with a *de novo* designed three-stranded coiled-coil domain that features a Cys_3 layer to accommodates two Cu(I) ions among its three Cys residues [55]. In that study, at neutral pH's spectral changes were linear through the addition of 2 copper equivalents, while spectral changes were clearly biphasic at pH 9, supporting the formation of distinct Cu and Cu_2 complexes at elevated pH. The pH dependence of the binding mode was confirmed by XAS, and shows that cooperative versus sequential binding can be dependent on subtle changes in environment.

It is generally accepted that, under normal cellular conditions, little to no unbound copper is present, and copper pools are stored in metallothionein and/or in complex with other biological chelators such as glutathione (GSH) [56]. To better mimic cellular conditions, we repeated the addition of Cu(I) to XIAP-RING-W and Mag-Fura-2 in the presence of 0.2 mM glutathione and recorded the change in spectral features as a function of time. Most of the bound zinc is released within 90 min., indicating that even in the presence of endogenous copper chelators, disruption of the zinc binding sites by added copper is observed.

Finally, to estimate the relative affinity of RING for copper and zinc, the data in Figure 2 were fit to a binding isotherm while considering ligand depletion (given in experimental section) to yield an equilibrium constant K_{obs} of 0.6 ± 0.4 μM (Figure S6). Owing to the presence of bound Zn, however, this value

constitutes the equilibrium constant for the reaction below, wherein n = number of Cu(I) ions bound, rather than for the dissociation of copper from the protein:

$$2Zn(II) + Cu_nRING \rightarrow nCu(I) + Zn_2RING$$

The relative affinity of XIAP-RING-W for Cu and Zn (K_{CU}/K_{Zn}) wherein K_{Cu} and K_{Zn} represent the *average* affinity constants (per metal ion) for copper and zinc, respectively, can be calculated from equation (1) (derivation in Figure S7):

$$K_{obs}^{-1} = \left(\frac{K_{Cu}}{K_{Zn}}\right)^{n-2} \qquad (1)$$

Therefore, assuming per titration data above that 5-6 ions of Cu(I) are bound, the relative affinity ranges between ~ 10^1-10^2, indicating that on a per metal ion basis, Cu(I) is the thermodynamically favored metal.

The results herein show that XIAP-RING-W binds multiple Cu(I) ions per zinc binding site, and that the binding of copper ions is accompanied by a release of protein-bound zinc, even in the presence of glutathione. While the binding of multiple copper ions at the cysteine rich zinc binding domain is consistent with other reports and the known ability of sulfur-rich binding sites to support multiple Cu(I) ions, no clear patterns have emerged that correlate ZF structure with copper loading. For example, we have previously shown that Cu(I) binds to the ZF consensus peptides (CP) that adopt the classical ZF $\beta\beta\alpha$ secondary structural motif but vary in the number of Cys residues at the Zn(II) binding site, and that the number of bound copper ions increases as the number of Cys residues increases. Specifically, full and stoichiometric displacement of Co(II), used as a spectroscopic surrogate for Zn(II), was complete upon addition of 2 and 3 Cu(I) equivalents to Co(II)CP-CCHC and Co(II)CP-CCCC respectively, indicating that thiol-rich binding sites can accommodate multiple Cu(I) ions [37] and providing precedent for the stoichiometries observed above for XIAP-RING-W. Similarly, tristetraproline, which features six cysteine residues that span two separate zinc binding sites, was found to bind a total of three Cu(I) ions per protein [38]. In contrast, the recent characterization of Cu(I) interactions with the RNF11 RING domain indicate only one Cu(I) binds per Zn(II) binding site, despite the presence of six cysteine residues in the metal binding region. This resulting 2:1 Cu:RING stoichiometry contrasts with the ~5:1 stoichometry we observe for XIAP-RING-W herein, highlighting the differences in copper binding properties of zinc-structural proteins, even for those within the same family. Native and designed Cu(I) binding proteins also feature diversity with respect to copper binding stoichiometry. For example, cellular copper chaperones such as AtoxI utilize two cysteine residues

to transport a single Cu(I) ion [1], while the yeast Ctr1 copper transporter utilizes six Cys residues to bind up to four Cu(I) ions [57]. Similarly, as noted above, a *de novo* designed three-stranded coiled-coil domain that features a Cys_3 layer accommodates two Cu(I) ions among its three Cys residues [55]. Finally, metallothioneins (MTs) feature thiol rich binding sites that accommodate multiple equivalents of Cu(I), Zn(II), and/or Cd(II). For example, the well-characterized mammalian MTs feature 20 Cys residues that bind 12 Cu(I) ions in the thermodynamically preferred stoichiometry, but can achieve stoichiometries as high as 20, known as "supermetallation" [58, 59]. These examples of copper binding at both ZF sites and within known copper binding proteins demonstrate the diverse and variable nature of biological copper-thiolate coordination motifs. Further investigation of copper interactions with diverse zinc structural sites is needed to elucidate possible correlation of bound copper ions with protein structure.

Impact of Cu(I) binding on XIAP-RING-W structure

Many RING domains, including XIAP-RING, form homo-dimeric structures, and amino acid mutations that disrupt dimer formation also abolish E3 ligase activity [45, 50]. If Cu(I) substitution of Zn(II) induces significant changes in the coordination geometry at the metal-binding sites, it is possible that RING-finger dimerization would be impacted, and by extension, so would RING function. Therefore, the ability of Cu(I) to influence dimer formation was assessed via analytical size-exclusion chromatography. As shown in Figure 4 and Table 1, isolated XIAP-RING-W protein exists primarily as a dimeric protein, as evidenced by a single peak that correlates well with the expected mass of a dimeric RING-W complex. Upon addition of increasing amounts of Cu(I) the peak broadens and shifts to a larger elution volume that correlates to a smaller size, indicating loss of the dimeric structure. To ensure that the loss of dimeric structure is owing to addition of Cu(I), multiple controls were performed. Chromatograms of XIAP-RING-W recorded in the absence and presence of 30 % acetonitrile ensure that the observed structural changes are not owing to added acetonitrile form the Cu(I) stock solution (Figure S8). 2 mM ascorbate was included to ensure Cu(I) remains reduced under the ambient conditions of the experiment, and control experiments utilizing the Cu(I) specific

Table 1. Observed molecular weights of XIAP-RING-W variants as determined by analytical size exclusion measurements.

Protein	**MW_{calc} (kD)**	**MW_{obs} (kD**
RING-W	16.3	17.4 ± 0.3
RING-W_V461E	8.19	11.94 ± 0.05
RING-W + 7 eq. Cu(I)	N/A	12.3 ± 0.2

probe BCA show that Cu(I) in the presence of ascorbate is stable throughout the course of the experiment (Figure S9). Although the Cu-RING complex and ascorbate will separate during the chromatography, the thiol-rich binding sites are likely to stabilize the Cu(I) oxidation state. To support this, 10 μM XIAP-RING_W was incubated with 50 μM Cu(I) in degassed buffer and subsequently exposed to ambient conditions. The resulting absorbance spectrum was stable over the course of one hour, indicating that the Cu(I)-thiolate motif stays intact during the time-frame of the experiment (Figure S10).

For comparison, we also prepared a construct of XIAP-RING-W that contains the mutation V461E that has previously been shown to disrupt the dimeric RING structure, resulting in stable monomeric protein. As shown in Table 1, the observed size of XIAP-RING-W in the presence of 7 eq. Cu(I) correlates well with the monomeric V461E mutant protein, providing further evidence that the addition of Cu(I) that results in a concomitant loss of Zn(II) binding also results in loss of dimeric structure and likely produces monomeric RING. Moreover, the addition of 3.5 eq. of Cu(I) results in a mixture of monomeric and dimeric structures, providing further evidence that multiple Cu(I) ions are required to fully disrupt the Zn_2RING structure. Given the demonstrated importance of dimeric structure for proper RING ubiquitination activity, it is highly likely that Cu(I) induced Zn(II) release is also accompanied by a loss of function.

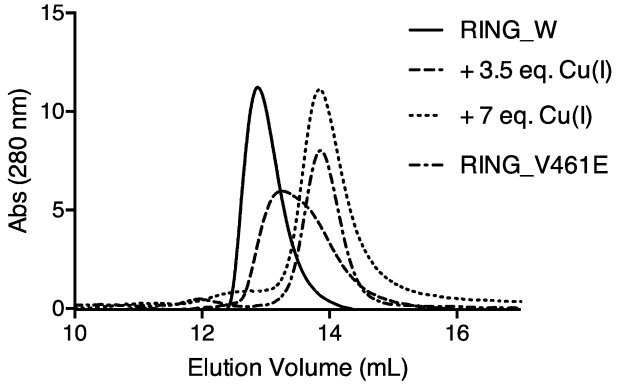

Figure 4. Analytical size exclusion chromatograms of 42 μM XIAP-RING-W constructs in the presence of Cu(I) as indicated.

Conclusion

We show herein that the RING finger domain of the XIAP protein binds multiple equivalents of copper, resulting in Zn(II) ejection. Moreover, we have demonstrated that copper affinity for the RING domain is high enough to cause zinc displacement even in the presence of cellular concentrations of glutathione, providing a biological basis for the interaction. Binding of Cu(I) to XIAP-RING and disruption of the dimeric structure reveals that elevated copper concentrations may have a functional impact and provide a molecular basis for attenuated XIAP ubiquitination activity in the presence of copper. The resulting

disruption of RING finger structure, and by extension, likely function, described here adds to the growing body of literature described in the introduction that shows Cu(I) can efficiently disrupt ZF domains.

As noted above, the work described herein constitutes the second example of an investigation of copper-RING domain interactions, the first being studies by Wang et al. on the RING finger domain of RNF11 [49]. Over 600 RING domains have been identified in the human genome, and while all RING domains share the unique bi-nuclear zinc-binding structure, diversity in other characteristics within the family are observed [60] . Most RING domains are shown to be E3 ligases, including XIAP-RING [50]. However, RNF-11 was recently proposed to regulate ubiquitination by binding E2-Ubiquitin constructs tightly while displaying minimal E3 ligase activity [61]. Moreover, many RING domains function as homodimers, while others, including RNF-11, maintain activity as a monomeric protein [45], [61]. These biochemical and functional differences may give rise to differential impact of copper and protein structure and function. While Cu(I) is able to displace Zn(II) from both XIAP-RING and RNF-11, copper binds with a higher stoichiometry to XIAP-RING. While the difference in stoichiometry is not at this time clear, as noted above, copper-thiolate interactions display a range of coordination geometries and stoichiometries. Moreover, despite the differences in functional quaternary structure between the two proteins, copper results in disruption of structure for both but with a different impact: disruption of dimeric structure for XIAP and protein oligomerization for RNF-11. Taken together the work shows how even among proteins within the same family and with similar function, functional differences in the impact of copper may be seen.

Acknowledgements

This work was supported by the National Science Foundation (#CHE-1807773 to K.E.S.) and Macalester College.

Supplementary Material

Full sequence of XIAP-RING-W, mass spectral data, uncorrected absorption spectra, spectral response of Magfura-2 to Cu(I) and Zn(II), fitting of data for relative affinity constants, impact of acetonitrile on SEC experiments, stability of Cu(I) and Cu(I)-RING protein under ambient conditions.

Statements and declarations: The authors have no relevant financial or non-financial interests to disclose.

References

1 A. K. Boal and A. C. Rosenzweig (2009) Chem Rev 109:4760-4779
2 J. H. Kaplan and S. Lutsenko (2009) Journal of Biological Chemistry 284:25461-25465
3 N. J. Robinson and D. R. Winge (2010) Annu Rev Biochem 79:537-562
4 L. Macomber and J. A. Imlay (2009) P Natl Acad Sci USA 106:8344-8349
5 P. Tsvetkov, S. Coy, B. Petrova, M. Dreishpoon, A. Verma, M. Abdusamad, J. Rossen, L. Joesch-Cohen, R. Humeidi, R. D. Spangler, J. K. Eaton, E. Frenkel, M. Kocak, S. M. Corsello, S. Lutsenko, N. Kanarek, S. Santagata and T. R. Golub (2022) Science 375:1254-1261
6 C. J. Chang (2015) Nat Chem Biol 11:744-747
7 D. C. Brady, M. S. Crowe, M. L. Turski, G. A. Hobbs, X. Yao, A. Chaikuad, S. Knapp, K. Xiao, S. L. Campbell, D. J. Thiele and C. M. Counter (2014) Nature 509:492-496
8 E. J. Ge, A. I. Bush, A. Casini, P. A. Cobine, J. R. Cross, G. M. DeNicola, Q. P. Dou, K. J. Franz, V. M. Gohil, S. Gupta, S. G. Kaler, S. Lutsenko, V. Mittal, M. J. Petris, R. Polishchuk, M. Ralle, M. L. Schilsky, N. K. Tonks, L. T. Vahdat, L. Van Aelst, D. Xi, P. Yuan, D. C. Brady and C. J. Chang (2022) Nat Rev Cancer 22:102-113
9 J. M. Berg and H. A. Godwin (1997) Annu Rev Biophys Biomol Struct 26:357-371
10 J. M. Berg and D. L. Merkle (1989) J Am Chem Soc 111:3759-3761
11 J. M. Berg and Y. Shi (1996) Science 271:1081-1085
12 J. H. Laity, B. M. Lee and P. E. Wright (2001) Curr Opin Struc Biol 11:39-46
13 L. Decaria, I. Bertini and R. J. P. Williams (2010) Metallomics 2:706-709
14 S. J. Lee and S. L. J. Michel (2014) Accounts Chem Res 47:2643-2650
15 J. C. Payne, M. A. t. Horst and H. A. Godwin (1999) J Am Chem Soc 121:6850-6855
16 R. C. diTargiani, S. J. Lee, S. Wassink and S. L. Michel (2006) Biochemistry 45:13641-13649
17 B. A. Krizek and J. M. Berg (1992) J Am Chem Soc 31:2984-2986
18 J. E. P. Brandis, S. M. Zalesak, M. A. Kane and S. L. J. Michel (2021) Inorg Chem 60:7697-7707
19 J. L. Michalek, S. J. Lee and S. L. J. Michel (2012) J Inorg Biochem 112:32-38
20 B. A. Krizek, D. L. Merkle and J. M. Berg (1993) Inorg Chem 32:937-940
21 W. Bal, T. Schwerdtle and A. Hartwig (2003) Chem Res Toxicol 16:242-248
22 Z. Lai, D. A. Freedman, A. J. Levine and G. L. McLendon (1998) Biochemistry 37:17005-17015
23 J. C. Payne, B. W. Rous, A. L. Tenderholt and H. A. Godwin (2003) Biochemistry 42:14214-14224
24 P. C. Roehm and J. M. Berg (1997) Biochemistry 36:10240-10245
25 M. Asmuss, L. H. Mullenders, A. Eker and A. Hartwig (2000) Carcinogenesis 21:2097-2104
26 A. Hartwig, M. Asmuss, I. Ehleben, U. Herzer, D. Kostelac, A. Pelzer, T. Schwerdtle and A. Burkle (2002) Environ Health Perspect 110 Suppl 5:797-799
27 T. W. Hutchens, M. A. Allen, C. M. Li and T.-T. Yip (1992) FEBS Lett 309:170-174
28 P. F. Predki and B. Sarkar (1992) J Biol Chem 267:5842-5846
29 M. A. Franzman and A. M. Barrios (2008) Inorg Chem 2008:3928-3930
30 J. L. Larabee, J. R. Hocker and J. S. Hanas (2005) Chem Res Toxicol 18:1943-1954
31 K. Ok, W. Li, H. M. Neu, S. Batelu, T. L. Stemmler, M. A. Kane and S. L. J. Michel (2020) Chem - Eur J 26:1535-1547
32 G. Park, Z. N. Amaris, M. K. Eiken, K. V. Baumgartner, K. A. Johnston, M. A. Williams, J. G. Marckwordt, J. E. Millstone, K. E. Splan and K. E. Wheeler (2019) Environ Sci: Nano 6:2367-2378
33 K. Kluska, M. D. Peris-Diaz, D. Plonka, A. Moysa, M. Dadlez, A. Deniaud, W. Bal and A. Krezel (2020) Chem Commun (Cambridge, U K) 56:1329-1332
34 K. Kluska, G. Veronesi, A. Deniaud, B. Hajdu, B. Gyurcsik, W. Bal and A. Krezel (2022) Angew Chem, Int Ed 61:e202116621
35 C. Abbehausen (2019) Metallomics 11:15-28
36 S. M. Quintal, Q. A. dePaula and N. P. Farrell (2011) Metallomics 3:121-139
37 R. T. Doku, G. Park, K. E. Wheeler and K. E. Splan (2013) J Biol Inorg Chem 18:669-678

38 G. D. Shimberg, K. Ok, H. M. Neu, K. E. Splan and S. L. J. Michel (2017) Inorganic Chemistry 56:6838-6848
39 S. M. Yuan, S. M. Chen, Z. Y. Xi and Y. Z. Liu (2017) Metallomics 9:1169-1175
40 F. Sommer, J. Kropat, D. Malasarn, N. E. Grossoehme, X. H. Chen, D. P. Giedroc and S. S. Merchant (2010) Plant Cell 22:4098-4113
41 S. Narindrasorasak, P. Kulkarni, P. Deschamps, Y. M. She and B. Sarkar (2007) Biochemistry 46:3116-3128
42 B. Sarkar and E. A. Roberts (2011) Metallomics 3:20-27
43 Y. Liang, P. M. Ewing, W. J. Laursen, V. T. Tripp, S. Singh and K. E. Splan (2014) J Inorg Biochem 140:104-110
44 S. N. Chen, T. Fang, J. Y. Kong, B. B. Pan and X. C. Su (2019) Sci Rep 9:7428
45 R. Budhidarmo, Y. Nakatani and C. L. Day (2012) Trends Biochem Sci 37:58-65
46 K. L. B. Borden and P. S. Freemont (1996) Curr Opin Struc Biol 6:395-401
47 A. J. Saurin, K. L. B. Borden, M. N. Boddy and P. S. Freemont (1996) Trends in Biochem Sci 21:208-214
48 Y. Yang, S. Y. Fang, J. P. Jensen, A. M. Weissman and J. D. Ashwell (2000) Science 288:874-877
49 Y. Wang, H. Hu, S. Yuan, Y. Li, K. Cao, H. Sun and Y. Liu (2022) Inorganic Chemistry Frontiers 9:3820-3827
50 Y. Nakatani, T. Kleffmann, K. Linke, S. M. Condon, M. G. Hinds and C. L. Day (2013) Biochem J 450:629-638
51 A. Badarau and C. Dennison (2011) P Natl Acad Sci USA 108:13007-13012
52 V. Sivo, G. D'Abrosca, I. Baglivo, R. Iacovino, P. V. Pedone, R. Fattorusso, L. Russo, G. Malgieri and C. Isernia (2019) Inorg Chem 58:1067-1080
53 Z. G. Xiao, J. Brose, S. Schimo, S. M. Ackland, S. La Fontaine and A. G. Wedd (2011) Journal of Biological Chemistry 286:11047-11055
54 T. Liu, A. Ramesh, Z. Ma, S. K. Ward, L. Zhang, G. N. George, A. M. Talaat, J. C. Sacchettini and D. P. Giedroc (2007) Nat Chem Biol 3:60-68
55 T. B. J. Pinter, C. S. Ervin, A. Deb, J. E. Penner-Hahn and V. L. Pecoraro (2022) Inorg Chem 61:5084-5091
56 T. D. Rae, P. J. Schmidt, R. A. Pufahl, V. C. Culotta and T. V. O'Halloran (1999) Science 284:805-808
57 Z. G. Xiao, F. Loughlin, G. N. George, G. J. Howlett and A. G. Wedd (2004) J Am Chem Soc 126:3081-3090
58 D. E. Sutherland and M. J. Stillman (2011) Metallomics 3:444-463
59 A. Krezel and W. Maret (2021) Chem Rev 121:14594-14648
60 R. J. Deshaies and C. A. Joazeiro (2009) Annu Rev Biochem 78:399-434
61 R. Budhidarmo, J. Zhu, A. J. Middleton and C. L. Day (2018) Febs Lett 592:1434-1444